FUNDAMENTALS OF METAL FATIGUE ANALYSIS

Julie A. Bannantine, Ph.D.
University of Illinois

Jess J. Comer, Ph.D.
South Dakota School of Mines

James L. Handrock, Ph.D.
University of Illinois
Currently at Sandia National Labs.

Prentice Hall
Englewood Cliffs, New Jersey 07632

1

STRESS–LIFE

1.1 INTRODUCTION

The stress–life, S–N, method was the first approach used in an attempt to understand and quantify metal fatigue. It was the standard fatigue design method for almost 100 years. The S–N approach is still widely used in design applications where the applied stress is primarily within the elastic range of the material and the resultant lives (cycles to failure) are long, such as power transmission shafts. The stress–life method does not work well in low-cycle applications, where the applied strains have a significant plastic component. In this range a strain–based approach (Chapter 2) is more appropriate. The dividing line between low and high cycle fatigue depends on the material being considered, but usually falls between 10 and 10^5 cycles.

1.2 *S–N* DIAGRAM

The basis of the stress–life method is the Wöhler or S–N diagram, which is a plot of alternating stress, S, versus cycles to failure, N. The most common procedure for generating the S–N data is the rotating bending test. One example is the R. R. Moore test, which uses four-point loading to apply a constant moment to a rotating (1750 rpm) cylindrical hourglass-shaped specimen. This loading produces a fully reversed uniaxial state of stress. The specimen is mirror polished with a typical diameter in the test section of 0.25 to 0.3 in. The stress level at the surface of the specimen is calculated using the elastic beam equation ($S = Mc/I$) even if the resulting value exceeds the yield strength of the material.

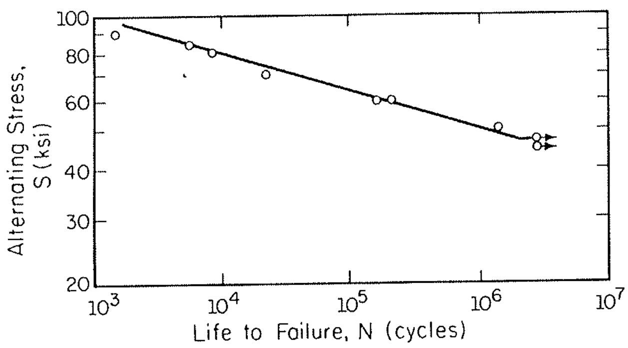

Figure 1.1 *S–N* curve for 1045 steel.

One of the major drawbacks of the stress–life approach is that it ignores true stress–strain behavior and treats all strains as elastic. This may be significant since the initiation of fatigue cracks is caused by plastic deformation (i.e., to–fro slip). The simplifying assumptions of the *S–N* approach are valid only if the plastic strains are small. At long lives most steels have only a small component of cyclic strain which is plastic (in some cases it is effectively too small to measure) and the *S–N* approach is valid.

S–N test data are usually presented on a log–log plot, with the actual *S–N* line representing the mean of the data. Certain materials, primarily body-centered cubic (BCC) steels, have an endurance or fatigue limit, S_e, which is a stress level below which the material has an "infinite" life (see Fig. 1.1). For engineering purposes, this "infinite" life is usually considered to be 1 million cycles. The endurance limit is due to interstitial elements, such as carbon or nitrogen in iron, which pin dislocations. This prevents the slip mechanism that leads to the formation of microcracks. Care must be taken when using the endurance limit since it can disappear due to:

1. Periodic overloads (which unpin dislocations)
2. Corrosive environments (due to fatigue corrosion interaction)
3. High temperatures (which mobilize dislocations)

It should be pointed out that the effect of periodic overloads mentioned above relates to smooth specimens. Notched components may have completely different behavior, due to the residual stresses set up by overloads. This is discussed more fully in Section 1.4.4.

Most nonferrous alloys have no endurance limit and the *S–N* line has a continuous slope (Fig. 1.2). A pseudo-endurance limit or fatigue strength for these materials is taken as the stress value corresponding to a life of 5×10^8 cycles.

There are certain general empirical relationships between the fatigue properties of steel and the less expensively obtained monotonic tension and hardness properties. When the *S–N* curves for several steel alloys are plotted in

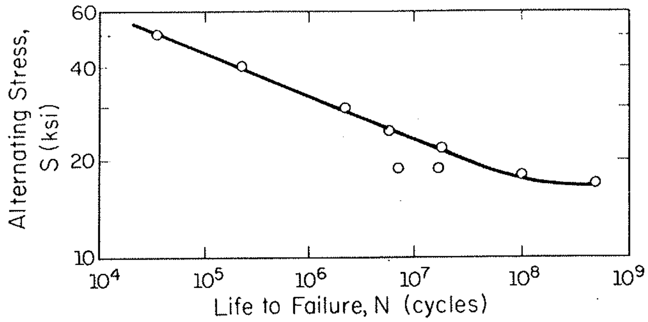

Figure 1.2 *S–N* curve for 2024-T4 aluminum. (Data from Ref. 1.)

nondimensional form using the ultimate strength, they tend to follow the same curve (Fig. 1.3).

The ratio of endurance limit to ultimate strength for a given material is the fatigue ratio (Fig. 1.4). Most steels with an ultimate strength below 200 ksi have a fatigue ratio of 0.5. It should be noted that this ratio can range from 0.35 to 0.6. Steels with an ultimate strength over 200 ksi often have carbide inclusions formed during the tempering of martensite. These nonmetallic inclusions serve as crack initiation points, which effectively reduce the endurance limit.

Using a rule of thumb relating hardness and ultimate strength [S_u(ksi) $\approx$ 0.5 $\times$ BHN], the following relationships for steel can be given:

Endurance limit related to hardness:

$$S_e(\text{ksi}) \approx 0.25 \times \text{BHN} \quad \text{for BHN} \leq 400 \qquad \text{if BHN} > 400,\ S_e \approx 100\ \text{ksi} \tag{1.1}$$

where BHN is the Brinell hardness number.

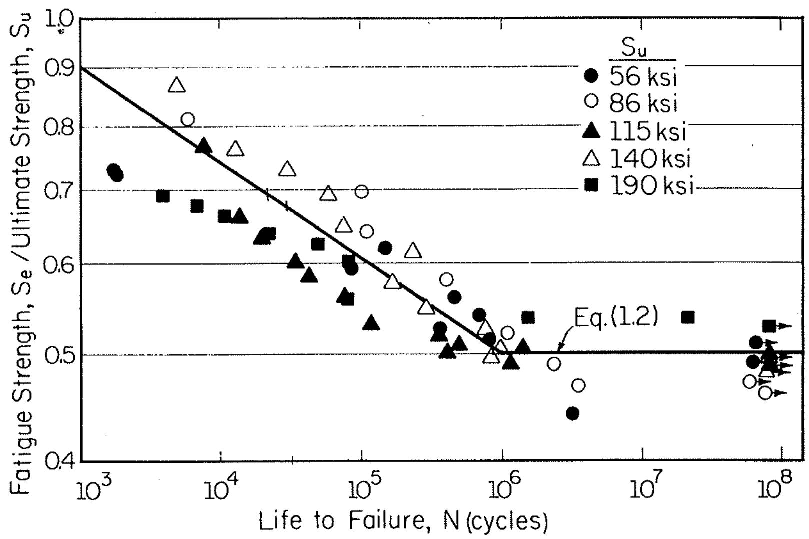

Figure 1.3 *S–N* curves for several wrought steels, plotted in ratio form (S_e/S_u).

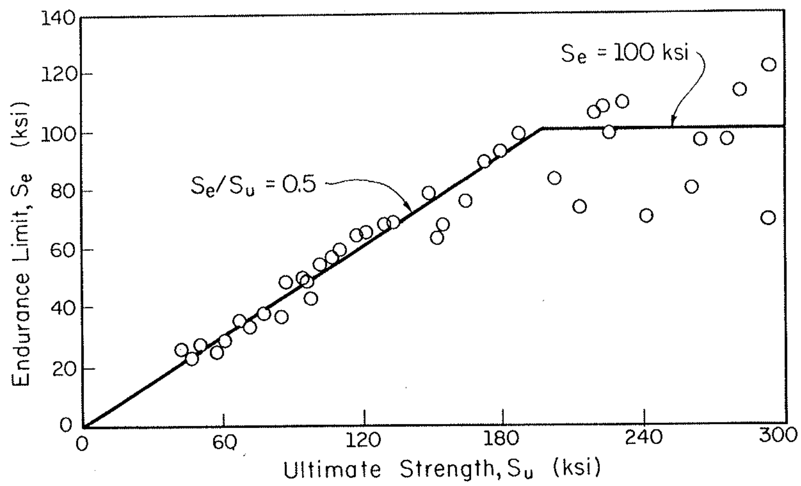

Figure 1.4 Relation between rotating bending endurance limit and tensile strength of wrought steels.

Endurance limit related to ultimate strength:

$$S_e \approx 0.5 \times S_u \quad \text{for } S_u \leq 200 \text{ ksi} \qquad \text{if } S_u > 200 \text{ ksi}, S_e \approx 100 \text{ ksi} \tag{1.2}$$

The alternating stress level corresponding to a life of 1000 cycles, S_{1000}, can be estimated as 0.9 times the ultimate strength. The line connecting this point and the endurance limit is the estimate used for the S–N design line (Fig. 1.5) if no actual fatigue data are available for the material.

In place of the graphical approach shown above, a power relationship can be used to estimate the S–N curve for steel:

$$S = 10^C N^b \quad (\text{for } 10^3 < N < 10^6) \tag{1.3}$$

where the exponents, C and b, of the S–N curve are determined using the two defined points shown in Fig. 1.5:

$$b = -\frac{1}{3}\log_{10}\frac{S_{1000}}{S_e} \qquad C = \log_{10}\frac{(S_{1000})^2}{S_e} \tag{1.4}$$

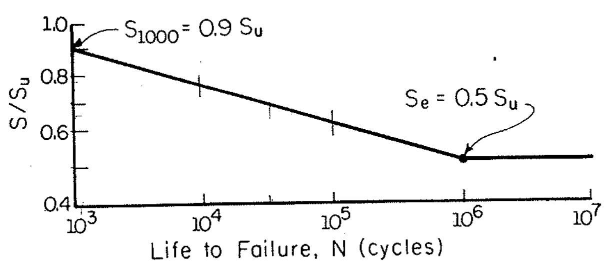

Figure 1.5 Generalized S–N curve for wrought steels on log–log plot.

The equation giving life in terms of an alternating stress is

$$N = 10^{-C/b} S^{1/b} \quad (\text{for } 10^3 < N < 10^6) \tag{1.5}$$

Note that when the estimates for S_{1000} and S_e are made,

$$S_{1000} \approx 0.9 S_u \quad \text{and} \quad S_e \approx 0.5 S_u \tag{1.6}$$

The S–N curve is defined as

$$S = 1.62 S_u N^{-0.085} \tag{1.7}$$

Similar empirical relationships for materials other than steel are not as clearly defined.

Before continuing, certain points about the S–N curve should be emphasized:

1. The empirical relationships outlined in this section are only estimates. Depending on the level of certainty required in the fatigue analysis, actual test data may be necessary.
2. The most useful concept of the S–N method is the endurance limit, which is used in infinite-life or "safe stress" designs.
3. In general, the S–N approach should not be used to estimate lives below 1000 cycles.

Regarding point 3, although there are several methods used to estimate the S–N curve in the range 1 to 1000 cycles they are not recommended. These methods use some percentage of ultimate strength, S_u, or true fracture stress, σ_f, as the estimate for alternating stress at either 1 or $\frac{1}{4}$ cycle. One of the main problems in using this approach is that most materials have an S–N curve which is very flat in the low cycle region. This is due to the large plastic strains caused by high load levels. When doing low cycle analysis a strain-based approach is more appropriate.

1.3 MEAN STRESS EFFECTS

The following relationships and definitions are used when discussing mean and alternating stresses (Fig. 1.6):

$$\Delta\sigma = \sigma_{\max} - \sigma_{\min} = \text{stress range}$$

$$\sigma_a = \frac{\sigma_{\max} - \sigma_{\min}}{2} = \text{stress amplitude}$$

$$\sigma_m = \frac{\sigma_{\max} + \sigma_{\min}}{2} = \text{mean stress}$$

$$R = \frac{\sigma_{\min}}{\sigma_{\max}} = \text{stress ratio} \qquad A = \frac{\sigma_a}{\sigma_m} = \text{amplitude ratio}$$

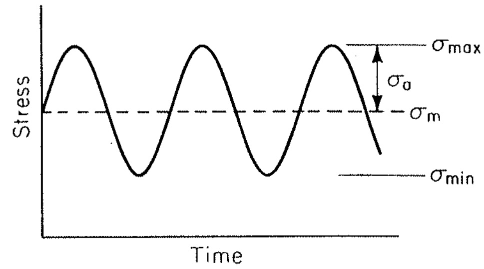

Figure 1.6 Terminology for alternating stress.

The R and A values corresponding to several common loading situations are:

Fully reversed:	$R = -1$	$A = \infty$
Zero to max:	$R = 0$	$A = 1$
Zero to min:	$R = \infty$	$A = -1$

The results of a fatigue test using a nonzero mean stress are plotted on a Haigh diagram (alternating stress versus mean stress) with lines of constant life drawn through the data points (Fig. 1.7). This diagram is sometimes incorrectly called the modified Goodman diagram. The data can also be plotted on a master diagram (Fig. 1.8) which has an extra set of axes for maximum and minimum stress.

Since the tests required to generate a Haigh diagram can be expensive, several empirical relationships have been developed to generate the line defining the infinite-life design region. These methods use various curves to connect the endurance limit on the alternating stress axis to either the yield strength, S_y, ultimate strength, S_u, or true fracture stress, σ_f, on the mean stress axis.

The following relationships are commonly used and are shown on Fig. 1.9:

$$\text{Soderberg (USA, 1930):} \quad \frac{\sigma_a}{S_e} + \frac{\sigma_m}{S_y} = 1 \tag{1.8}$$

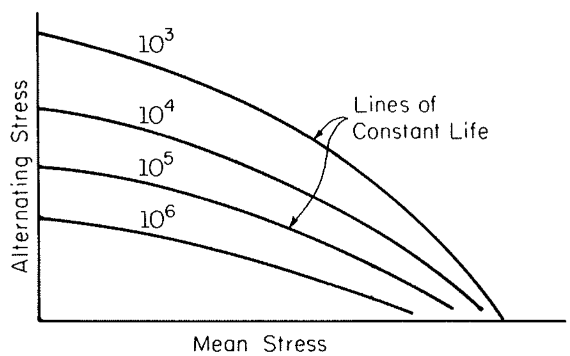

Figure 1.7 Haigh diagram.

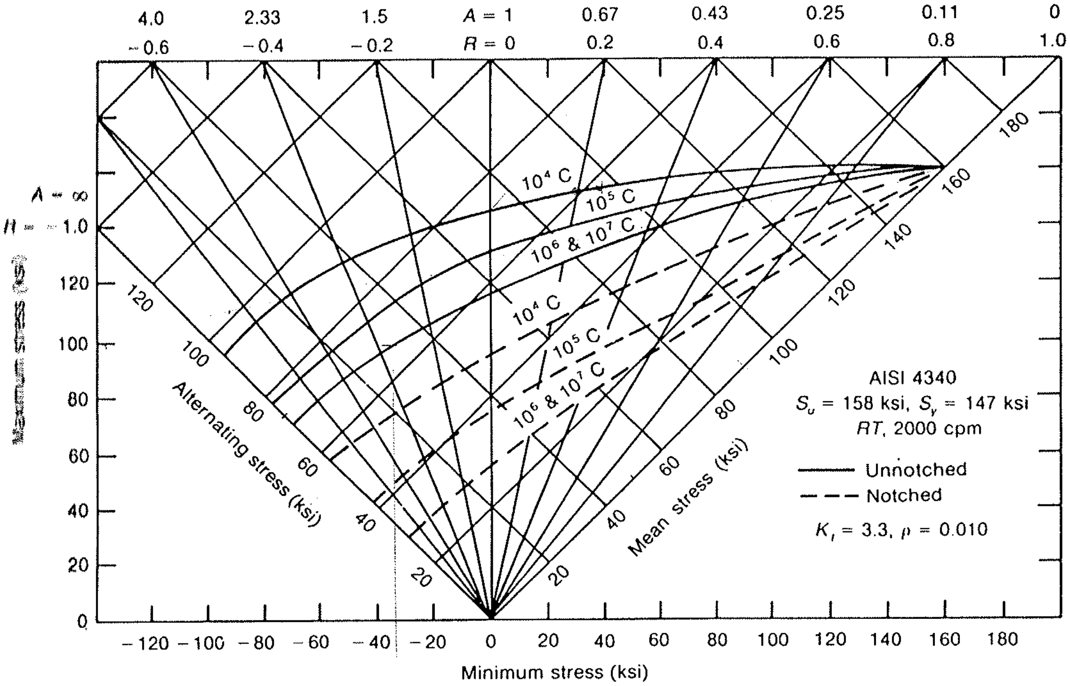

Figure 1.8 Master diagram for AISI 4340 steel. (From Ref. 2.)

$$\text{Goodman (England, 1899):} \quad \frac{\sigma_a}{S_e} + \frac{\sigma_m}{S_u} = 1 \tag{1.9}$$

$$\text{Gerber (Germany, 1874):} \quad \frac{\sigma_a}{S_e} + \left(\frac{\sigma_m}{S_u}\right)^2 = 1 \tag{1.10}$$

$$\text{Morrow (USA, 1960s):} \quad \frac{\sigma_a}{S_e} + \frac{\sigma_m}{\sigma_f} = 1 \tag{1.11}$$

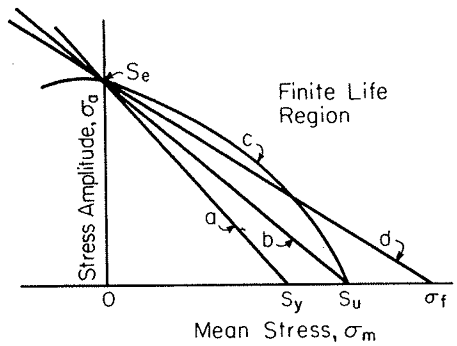

Figure 1.9 Comparison of mean stress equations (a. Soderberg, b. Goodman, c. Gerber, d. Morrow).

The following generalizations can be made when discussing cases of tensile mean stress:

1. The Soderberg method is very conservative and seldom used.
2. Actual test data tend to fall between the Goodman and Gerber curves.
3. For hard steels (i.e., brittle), where the ultimate strength approaches the true fracture stress, the Morrow and Goodman lines are essentially the same. For ductile steels ($\sigma_f > S_u$) the Morrow line predicts less sensitivity to mean stress.
4. For most fatigue design situations, $R < 1$ (i.e., small mean stress in relation to alternating stress), there is little difference in the theories.
5. In the range where the theories show a large difference (i.e., R values approaching 1), there is little experimental data. In this region the yield criterion may set design limits.

For finite-life calculations the endurance limit in any of the equations can be replaced with a fully reversed alternating stress level corresponding to that finite-life value.

Example 1.1

A component undergoes a cyclic stress with a maximum value of 110 ksi and a minimum value of 10 ksi. The component is made from a steel with an ultimate strength, S_u, of 150 ksi, an endurance limit, S_e, of 60 ksi, and a fully reversed stress at 1000 cycles, S_{1000}, of 110 ksi. Using the Goodman relationship, determine the life of the component.

Solution Determine the stress amplitude and mean stress.

$$\sigma_a = \frac{\sigma_{\max} - \sigma_{\min}}{2} = \frac{110 - 10}{2} = 50 \text{ ksi}$$

$$\sigma_m = \frac{\sigma_{\max} + \sigma_{\min}}{2} = \frac{110 + 10}{2} = 60 \text{ ksi}$$

Generate a Haigh diagram with constant life lines at 10^6 and 10^3 cycles. These lines are constructed by connecting the endurance limit, S_e, and S_{1000} values on the alternating stress axis to the ultimate strength, S_u, on the mean stress axis (see Fig. E1.1).

When the stress conditions for the component ($\sigma_a = 50$ ksi, $\sigma_m = 60$ ksi) are plotted on the Haigh diagram, the point falls between the 10^3 and 10^6 life lines. This indicates that the component will have a finite life, but the life is greater than 1000 cycles. Next, a line is drawn through the point representing the stress conditions and the ultimate strength, S_u, on the mean stress axis. This represents a constant life line at a life equal to the life of the component. This line intersects the fully reversed alternating stress axis at a value of 83 ksi. Note that this value could also be obtained by solving a modification of Eq. (1.9):

$$\frac{\sigma_a}{S_n} + \frac{\sigma_m}{S_u} = 1$$

cussing cases of tensile

ɔm used.
ınd Gerber curves.
:rength approaches the
ıes are essentially the
predicts less sensitivity

mean stress in relation
:heories.
'erence (i.e., R values
n this region the yield

of the equations can be
corresponding to that

n value of 110 ksi and a
a steel with an ultimate
and a fully reversed stress
onship, determine the life

:.

ksi

ksi

: 10^6 and 10^3 cycles. These
S_e, and S_{1000} values on the
mean stress axis (see Fig.

= 50 ksi, σ_m = 60 ksi) are
10^3 and 10^6 life lines. This
ıe life is greater than 1000
g the stress conditions and
ıresents a constant life line
tersects the fully reversed
lue could also be obtained

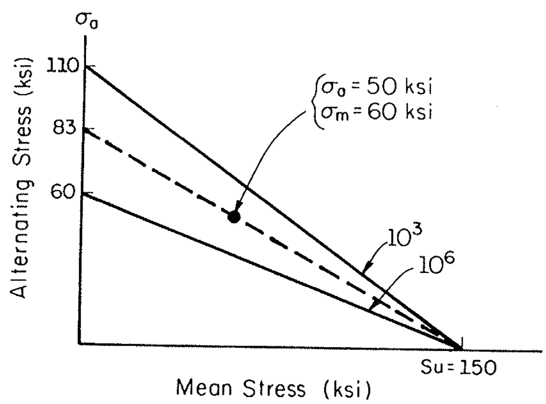

Figure E1.1 Haigh diagram.

where S_n is the fully reversed stress level corresponding to the same life as that obtained with the stress conditions σ_a and σ_m. For this problem,

$$\frac{50}{S_n} + \frac{60}{150} = 1$$

$$S_n = 83 \text{ ksi}$$

The value for S_n can now be entered on the S–N diagram (Fig. E1.2) to determine the life of the component, N_f. (Recall that the S–N diagram represents fully reversed loading). When a value of 83 ksi is entered on the S–N diagram for the material used for the component, the resulting life to failure, N_f, is 2.4×10^4 cycles.

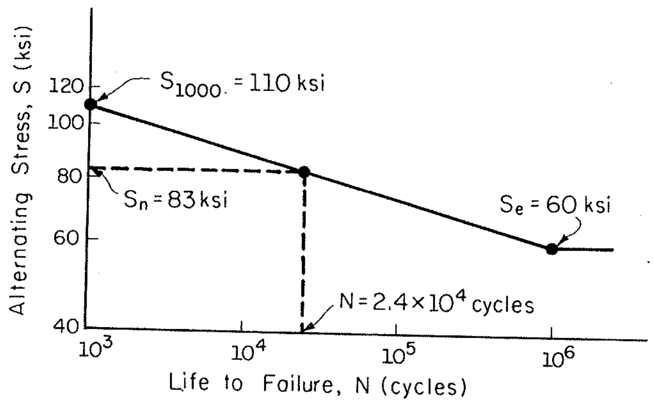

Figure E1.2 S–N diagram.

This problem could be redone using the Gerber [Eq. (1.10)], Soderberg [Eq. (1.8)], and Morrow [Eq. (1.11)] mean stress equations. Each technique would provide a slightly different life estimate.

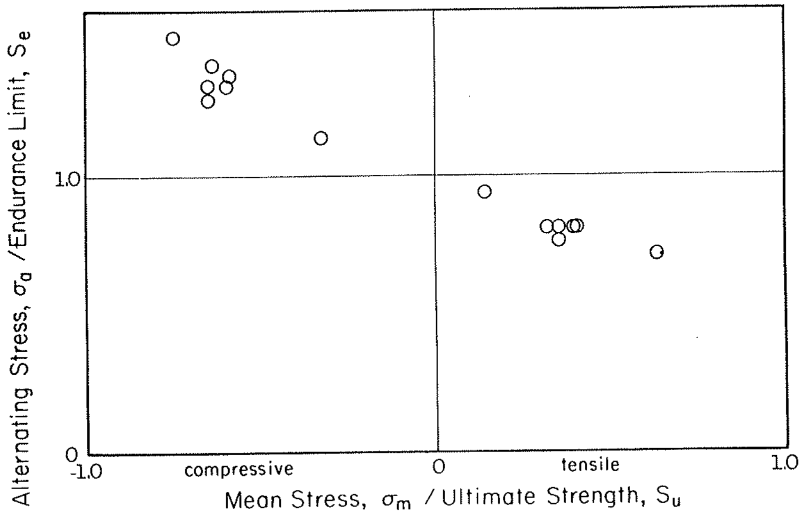

Figure 1.10 Compressive and tensile mean stress effect for smooth specimen. (Data from Ref. 3.)

As seen in Fig. 1.9, the three linear models predict that compressive mean stresses are very beneficial and allow for very large alternating stresses. Experimental results from smooth specimens do indeed indicate that a compressive mean stress is beneficial and increases the life at a given alternating stress (Fig. 1.10). There is difficulty in relating this behavior to notched components. The problems arise when trying to predict the residual stresses generated near the notch root. When extrapolating the Haigh diagram into the range of compressive mean stress, a conservative estimate for notched components is that a compressive mean stress has no effect (Fig. 1.11). At very large compressive mean stresses the design envelope will be set by yield or buckling limits.

Test results from torsion tests of unnotched specimens indicate that a mean shear stress has no effect on life when added to an alternating shear stress. This trend does not appear to hold for notched torsional components. The effect of a mean shear stress on an alternating normal stress is discussed in Chapter 7.

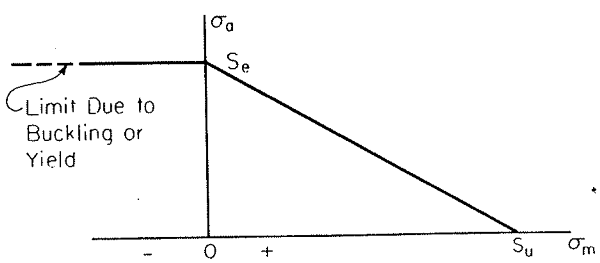

Figure 1.11 Estimate of Haigh diagram for notched components using Goodman line.

1.4 MODIFYING FACTORS

The results of an R. R. Moore test are from the special case of a mirror-polished 0.25 in diameter specimen loaded under fully reversed bending. To denote this, the endurance limit found using the R. R. Moore test is often given a prime, S_e'. The endurance limit needed for design situations, S_e, must take into account differences in size, surface finish, and so on.

For many years the emphasis of most fatigue testing was to gain an empirical understanding of the effects of various factors on the baseline S–N curves for ferrous alloys in the intermediate to long life ranges. The variables investigated include:

1. Size
2. Type of loading
3. Surface finish
4. Surface treatments
5. Temperature
6. Environment

The results of these tests have been quantified as modification factors which are applied to the baseline S–N data.

$$S_e = S_e' C_{\text{size}} C_{\text{load}} C_{\text{surf.fin.}} \cdots \tag{1.12}$$

This modified endurance limit tends to be conservative.

The modification factors are usually specified for the endurance limit, and the correction for the remainder of the S–N curve is not as clearly defined. The general trend is for these modification factors to have less effect at short lives. At the extreme limit of monotonic loading they all approach a value of 1. A conservative estimate is to use the modification factors on the entire S–N curve.

It is very important to remember that these modification factors are empirical models of a phenomenon and may give limited insight into the underlying physical processes. Great care must be taken when extrapolating these empirical modification factors beyond the range of data used to generate them.

1.4.1 Size Effects

The fatigue failure of a material is dependent on the interaction of a large stress with a critical flaw. In essence, fatigue is controlled by the weakest link of the material, with the probability of a weak link increasing with material volume. This differs from bulk material properties such as yield strength and modulus of elasticity. This phenomenon is evident in the fatigue test results of a material using specimens of varying diameters (see Table 1.1). The size effect has been correlated with the thin layer of surface material subjected to 95% or more of the

TABLE 1.1 Influence of Size on Endurance Limit

Diameter (in)	Endurance Limit (ksi)
0.3	33.0
1.5	27.6
6.75	17.3

Source: J. H. Faupel and F. E. Fisher, *Engineering Design,* John Wiley and Sons, New York, 1981. Reprinted with permission.

maximum surface stress. A large component will have a less steep stress gradient and hence a larger volume of material subjected to this high stress (Fig. 1.12). Consequently, there will be a greater probability of initiating a fatigue crack in large components. This concept is backed up by test results which show a less pronounced size effect for axial loading, where there is no gradient, than for bending or torsion. The idea of a highly stressed volume is important when considering stress gradients due to notches (see Chapter 4).

There are many empirical fits to the size effect data. A fairly conservative one is [5], in English units,

$$C_{\text{size}} = \begin{cases} 1.0 & \text{if } d \leq 0.3 \text{ in.} \\ 0.869d^{-0.097} & \text{if } 0.3 \text{ in.} \leq d \leq 10 \text{ in.} \end{cases} \tag{1.13}$$

and in SI units,

$$C_{\text{size}} = \begin{cases} 1.0 & \text{if } d \leq 8 \text{ mm} \\ 1.189d^{-0.097} & \text{if } 8 \text{ mm} \leq d \leq 250 \text{ mm} \end{cases} \tag{1.14}$$

where d is the diameter of the component. Some other points to consider when dealing with the size effect are:

1. The effect is seen mainly at very long lives.
2. The effect is small in diameters up to 2.0 in. even in bending or torsion.
3. Due to the processing problems inherent in large components, there is a greater chance of having residual stresses and various metallurgical variables, which may adversely affect fatigue strength.

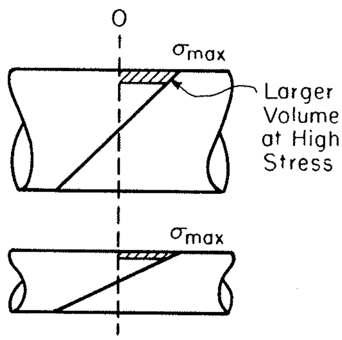

Figure 1.12 Stress gradient in large and small specimens.

The idea of critical volume can also be used to find a size modification factor for noncircular sections (see Ref. 5, p. 294).

1.4.2 Loading Effects

When relating the fatigue data from rotating bending and axial loading for a similar specimen, the volume idea discussed in the preceding section can be used. Since the axial specimen has no gradient, it has a greater volume of material subjected to the high stress. The ratio of endurance limits for a material found using axial and rotating bending tests ranges from 0.6 to 0.9. These test data may include some error due to eccentricity in axial loading. A conservative estimate is

$$S_e(\text{axial}) \approx 0.70 S_e(\text{bending}) \tag{1.15}$$

The ratio of endurance limits found using torsion and rotating bending tests ranges from 0.5 to 0.6. A theoretical value of 0.577 has been explained using the von Mises failure criterion. This relationship is discussed more thoroughly in Chapter 7. A reasonable estimate is

$$\tau_e(\text{torsion}) \approx 0.577 S_e(\text{bending}) \tag{1.16}$$

1.4.3 Surface Finish

The scratches, pits, and machining marks on the surface of a material add stress concentrations to the ones already present due to component geometry. Uniform fine-grained materials, such as high strength steel, are more adversely affected by a rough surface finish than a coarse-grained material such as cast iron.

The correction factor for surface finish is sometimes presented on graphs that use a qualitative description of surface finish such as "polished" or "machined" (Fig. 1.13). Some of the curves on this plot include effects other than

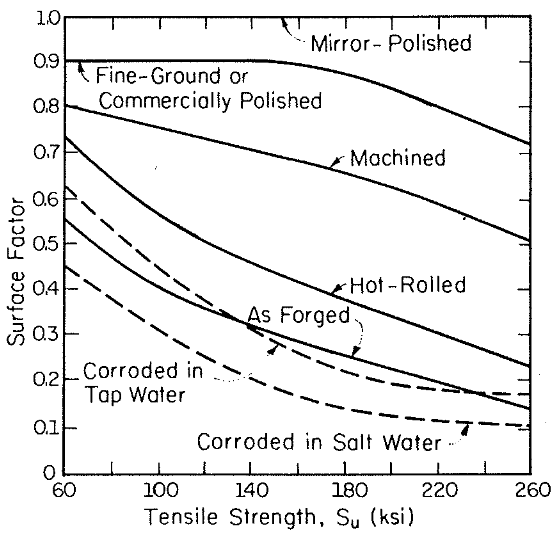

Figure 1.13 Surface finish factor: steel parts. (From Ref. 6.)

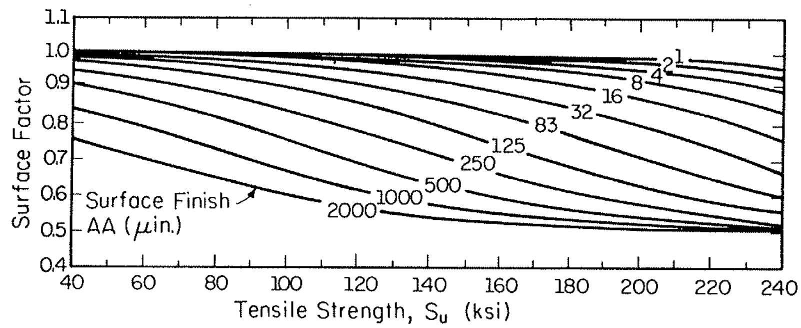

Figure 1.14 Surface finish factor versus surface roughness and strength: steel parts. (From Ref. 7.)

surface roughness. For example, the forged and hot-rolled curves include the effects of decarburization.

Other graphs, such as Fig. 1.14, use a quantitative measurement of surface roughness such as R_A, the root mean square or, AA, arithmetic average. The surface roughness resulting from various machining operations can be found in machining and manufacturing handbooks.

Some important points about the surface finish effect are:

1. The condition of the surface is more important for higher strength steels.
2. The residual surface stress caused by a machining operation can be important. An example is the residual tensile stress sometimes caused by some grinding operations.
3. At shorter lives, where crack propagation dominates, the condition of surface finish has less effect on the fatigue life.
4. Localized surface irregularities such as stamping marks can serve as very effective stress concentrations and should not be ignored.

1.4.4 Surface Treatment

Since fatigue cracks almost always initiate at a free surface, any surface treatment can have a significant effect on fatigue life. The effect of surface roughness from various forming operations was discussed in the preceding section. Other surface treatments can be categorized as plating, thermal, or mechanical. In all three cases the effect on fatigue life is due primarily to residual stresses.

As a review of residual stress, consider the unnotched beam (Fig. 1.15) subjected to a varying bending moment. The bending moment history is shown in Fig. 1.15d. If the simplifying assumption is made that the material is elastic–perfectly plastic, the history of the stress at the top surface of the beam is as shown in Fig. 1.15e.

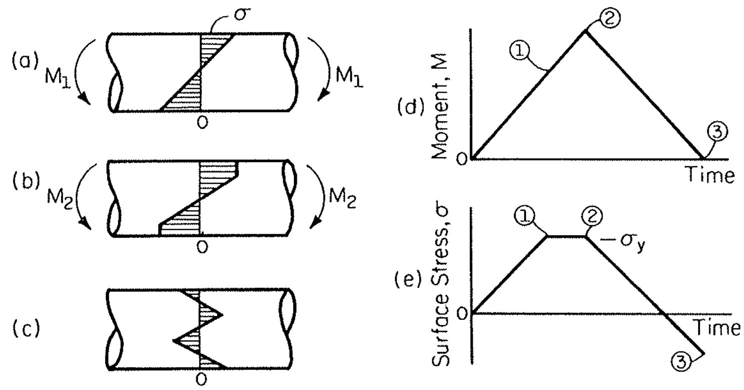

Figure 1.15 Residual stress in unnotched beam in bending.

1. At point 1 the surface of the beam is just at the point of yielding and the stress distribution is linear (Fig. 1.15a).
2. If the moment is increased to point 2, the outer layer of the beam begins to yield (Fig. 1.15b).
3. If the moment is reduced to point 3, the beam will have a residual stress distribution (Fig. 1.15c). When the outer layer of material yielded, it elongated and upon unloading the stresses and strains in the beam must meet compatibility and equilibrium requirements. Although the exact residual stress distribution is difficult to define, the important point is that the outer surface of the beam, which had yielded in tension, is now in residual compression.

Another example of residual stress is the notched member under axial loading, shown in Fig. 1.16. The loading history involves an initial tensile overload followed by fully reversed cyclic loads (Fig. 1.16d).

1. The initial overload (point 1) causes the material at the root of the notch to yield in tension (Fig. 1.16b) and when the load is released (point 2) this material will be in residual compression (Fig. 1.16c).
2. When the cyclic load is applied (points 3 and 4), the stress at the root of the notch will cycle between the limits shown on Fig. 1.16e.

Note that while the load is fully reversed, the stress at the root of the notch (where the fatigue crack will initiate) cycles about a compressive value. The residual stress in the material at the notch root has the same effect as an externally applied compressive mean stress of equal magnitude, and as pointed out in Section 1.3, this will increase life at a given alternating stress level. Remember that this discussion involves the residual mean stress in a notched member, not a mean stress due to an applied load.

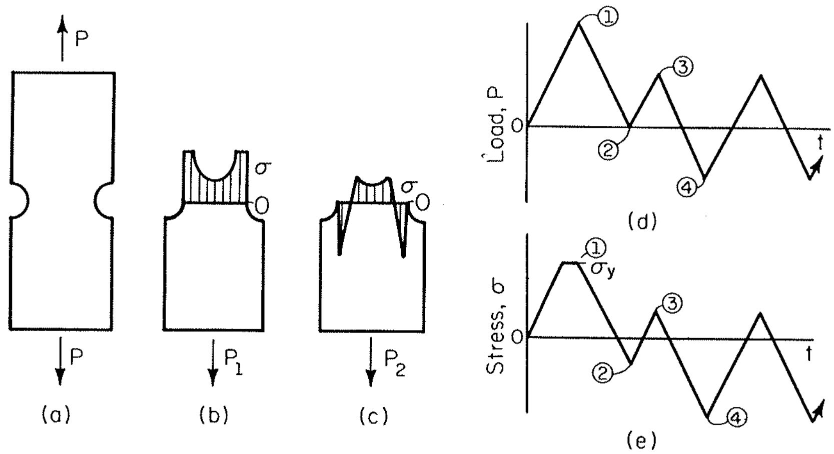

Figure 1.16 Residual stress in notched member under axial loading.

The method just described for producing a residual stress with an initial overload is called *prestressing* or *presetting*. An example of this is given in Table 1.2, which compares the endurance limit values of notched and unnotched plates of 4340 steel (S_u = 130 ksi). A comparison is also made of plates with and without an initial tensile overload. As can be seen, the preload sets up a residual stress which almost negates the effect of the notch.

Presetting is used on such components as coil and leaf springs. It should be noted that the initial overload on a component is favorable for future loading in the same direction as the overload, but unfavorable for loads in the opposite direction. For example, if a coil spring is preloaded in compression, it will have a beneficial effect only for future cyclic loading which is primarily in compression.

Presetting should not be used in cases of fully reversed loading. For example, the cold straightening of an axle shaft can reduce the endurance limit 20 to 50%.

In the following discussion on surface treatments it is important to keep these points in mind:

1. Since fatigue is a surface phenomenon, the residual stress at the surface of the material is critical.

TABLE 1.2 Endurance Limit of Plate with Hole under Axial Loading

	Endurance Limit (ksi)	
	Unnotched	Notched
No preload	58.0	23.0
With preload	56.6	53.7

Source: H. O. Fuchs and R. I. Stephens, *Metal Fatigue in Engineering*, John Wiley and Sons, New York, 1980. Reprinted with permission.

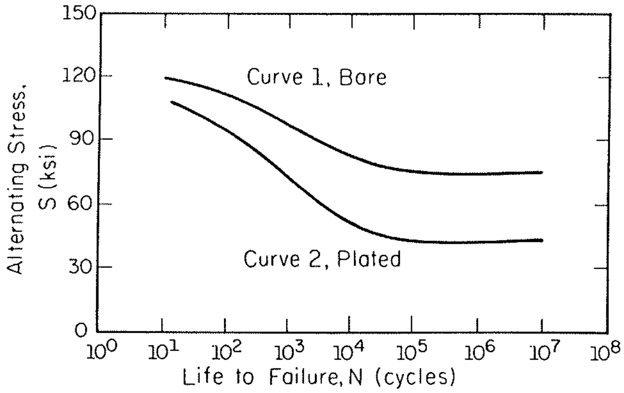

Figure 1.17 Effect of chrome plating on S–N curve of 4140 steel. (From Ref. 1.)

2. Compressive residual stresses are beneficial, and tensile stresses are detrimental to fatigue life.
3. Residual stresses are not always permanent, and various factors, such as high temperatures and overloads, may cause stress relaxation.

Plating. Chrome and nickel plating of steels can cause up to a 60% reduction in endurance limits (Figs. 1.17 and 1.18). This is due primarily to the high residual tensile stresses generated by the plating process. The following operations can help alleviate the residual tensile stress problem:

1. Nitride the part before plating.
2. Shot peen the part before or after plating.
3. Bake or anneal the part after plating.

Figure 1.19 shows the effect of shot peening a rotating beam specimen before and after a nickel-plating operation.

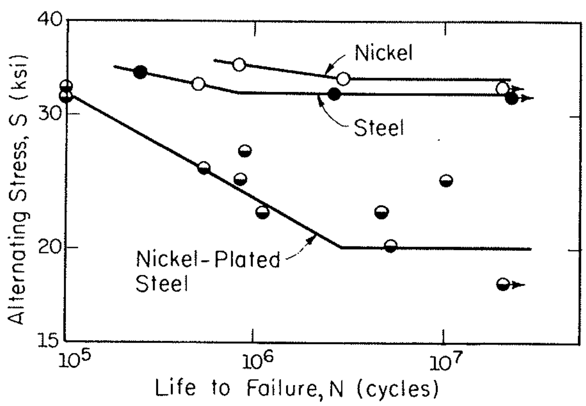

Figure 1.18 Effect of nickel plating on S–N curve of steel (S_u = 63 ksi). (From Ref. 9.)

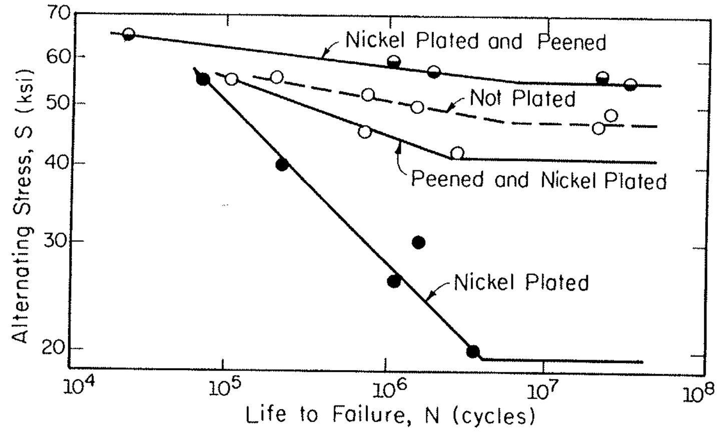

Figure 1.19 Effects of shot peening on S–N curve of nickel plated steel. (From Ref. 9.)

There are many factors involved with a plating operation which can affect fatigue life. The following are some general trends for chrome and nickel plating:

1. There is a greater reduction of fatigue strength as the yield strength of the material being plated increases.
2. The fatigue strength reduction due to plating is greater at longer lives.
3. The fatigue strength reduction is greater as the thickness of the plating increases.
4. It should also be noted that when fatigue occurs in a corrosive environment, the extra corrosion resistance offered by plating can more than offset the reduction in fatigue strength seen in a noncorrosive environment (see Table 1.7).

Plating with cadmium and zinc appear to have no effect on fatigue strength while still offering corrosion resistance. However, plating with these metals does not offer the wear resistance of chromium. It is important to remember that any electroplating operation can cause hydrogen embrittlement if the process is improperly controlled.

Thermal. Diffusion processes such as carburizing and nitriding are very beneficial for fatigue strength. These processes have the combined effect of producing a higher strength material on the surface as well as causing volumetric changes which produce residual compressive surface stresses. The effect of nitriding on notched steel members can be seen in Table 1.3.

Flame and induction hardening cause a phase transformation, which in turn causes a volumetric expansion. If these processes are localized to the surface, they produce a compressive residual stress which is beneficial for fatigue strength.

TABLE 1.3 Effect of Nitriding on Endurance Limit

	Endurance Limit (ksi)	
Geometry	Nitrided	Not Nitrided
Without notch	90	45
Half-circle notch	87	25
V notch	80	24

Source: Ref. 6.

Hot rolling and forging can cause surface decarburization. The loss of carbon atoms from the surface material causes it to have a lower strength and may also produce residual tensile stresses. Both of these factors are very detrimental to fatigue strength. The effect of decarburization on various high-strength steel alloys with notched and unnotched geometries can be seen in Table 1.4.

TABLE 1.4 Effect of Decarburization on Endurance Limit

		Endurance Limit (ksi)			
		Undecarburized		Decarburized	
Steel	S_u (ksi)	Smooth	Notched	Smooth	Notched
AISI 2340	250	122	69	35	25
AISI 2340	138	83	43	44	25
AISI 4140	237	104	66	31	22
AISI 4140	140	83	40	32	19

Source: Ref. 1.

Figure 1.20 shows the effect of forging on the endurance limit of steels with various tensile strengths. As can be seen, the endurance limit reduction for a low strength steel may only be a few percent, whereas there may be a five fold

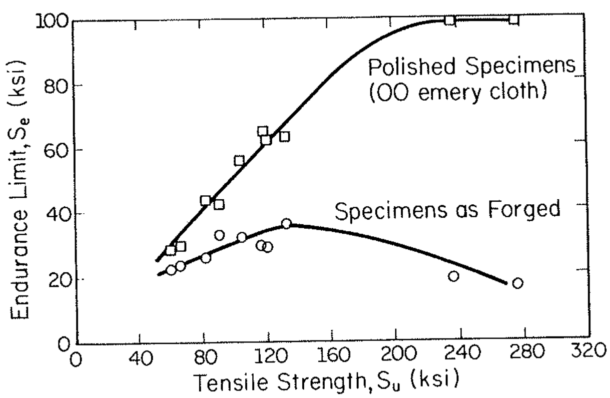

Figure 1.20 Effect of forging on the endurance limit of steels. (From Ref. 10.)

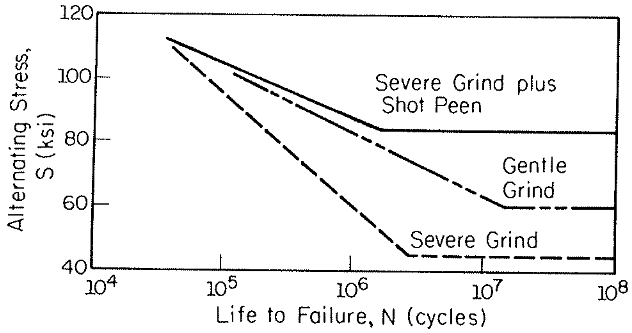

Figure 1.21 Effects of grinding on S–N curve of steel. (From Ref. 11.)

reduction for a high strength steel. This points out another general trend concerning the various surface factors that affect fatigue life. Almost all of these factors have a more pronounced influence as the strength of the base steel increases. In fact, for very low strength (i.e., lower carbon) steels, almost none of the factors will cause substantial increases or decreases in fatigue strength. In large part, this trend can be attributed to the ease with which residual stresses relax out of materials with low yield strengths.

It should also be noted that some manufacturing processes, such as welding, grinding, and flame cutting, can set up detrimental residual tensile stresses. Figure 1.21 shows the effect of gentle and severe grinding operations on the fatigue properties of a high strength steel (Rockwell C = 45). The figure also shows how shot peening can undo the damage caused by severe grinding.

Mechanical. There are several methods used to cold work the surface of a component to produce a residual compressive stress. The two most important are cold rolling and shot peening. Along with producing compressive residual stresses, these methods also work-harden the surface material. The great improvement in fatigue life is due primarily to the residual compressive stresses.

Cold rolling involves pressing steel rollers to the surface of a component which is usually rotated in a lathe. This method is used on large parts and can produce a deep residual stress layer. Figure 1.22 shows the effect of cold rolling. Another example of the benefits of cold rolling is the increased fatigue resistance of a bolt with rolled threads over one with cut threads (Table 1.5).

Shot peening is one of the most important methods of producing a residual compressive stress. This procedure involves blasting the surface of a component with high-velocity steel or glass beads. This puts the core of the material in residual tension and the skin in residual compression. The residual compressive stress layer is about 1 mm deep with a maximum value of about one-half the yield strength of the material. An example of the effect of shot peening is shown in Fig. 1.23.

One of the advantages of shot peening is the ease with which it can be used on oddly shaped parts such as coil springs. One disadvantage is that it leaves a

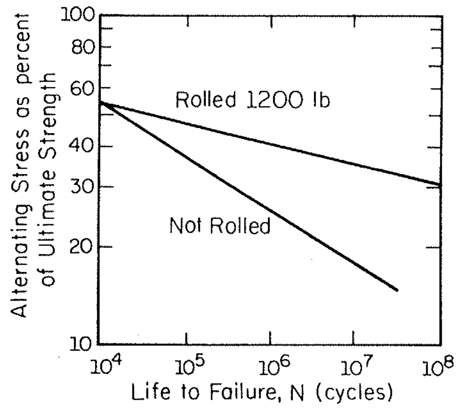

Figure 1.22 Effects of cold rolling on S–N curve of steel. (From Ref. 9.)

rough dimpled surface. If a smooth surface is required, a honing or polishing operation can be applied after the part is shot peened. This causes only a small reduction in fatigue strength.

Shot peening can be used to undo the deleterious effects caused by chrome

TABLE 1.5 Fatigue Strength at 10^5 cycles for Bolts (AISI 8635)[a]

	Fatigue Strength (ksi)
Rolled threads	74
Cut threads	44

[a] Bolts with the same thread design.

Source: H. O. Fuchs and R. I. Stephens, *Metal Fatigue in Engineering*, John Wiley and Sons, New York, 1980. Reprinted with permission.

and nickel plating (Fig. 1.19), decarburization, corrosion, and grinding (Fig. 1.21). It can also be used to great advantage on high-strength steels. As shown in Fig. 1.4, many steels with an ultimate strength above 200 ksi experience a

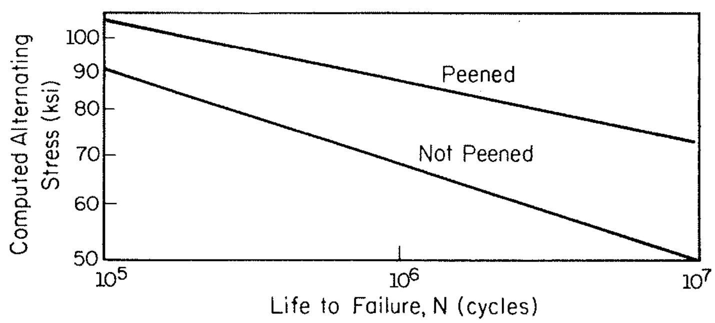

Figure 1.23 S–N curve of carburized gears in peened and unpeened conditions. (From Ref. 12.)

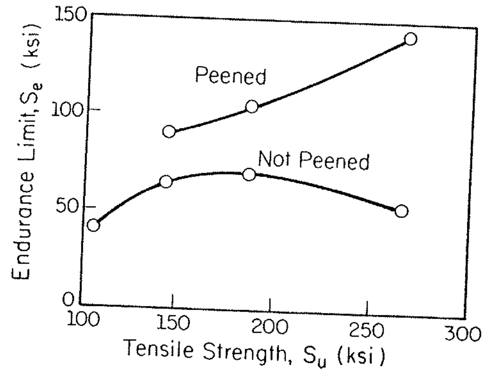

Figure 1.24 Effect of shot peening on endurance limit of high-strength steel. (From Ref. 13.)

reduction in endurance limit with increased strength. Figure 1.24 shows the effect of shot peening on the endurance limit of a high strength steel (0.45% C, 1.0% Mn, quenched and tempered). As can be seen, shot peening eliminates the roll-off in endurance limit, and a fatigue ratio of 0.5 is extended well beyond an ultimate strength of 200 ksi.

Some important points about cold working for residual compressive stresses are:

1. Cold rolling and shot peening have their greatest effect at long lives. At very short lives there is almost no improvement in the fatigue strength. At shorter lives the stress levels are high enough to cause yielding, which eliminates residual stresses.
2. Certain situations can cause the residual stresses to fade out or relax. These include high temperatures and overstressing. Approximate temperatures where this fading occurs are 500°F for steel and 250°F for aluminum.
3. Steels with yield strengths below 80 ksi are seldom cold rolled or shot peened. Due to their low yield points it is quite easy to introduce plastic strains that wipe out residual stresses.
4. A surface residual compressive stress has the greatest effect on fatigue life when it is applied to an area of the component where there is a stress gradient, primarily around notches.
5. It is possible to overpeen a surface. There is usually an optimum level for peening of a component, and more peening will actually begin to decrease fatigue strength.

Another point worth noting is that a high residual compressive stress at the surface of a material may cause subsurface fatigue failures. If the surface is in residual compression, to retain equilibrium the material below the surface must be in tension. When the stress distribution from the applied load is added to the residual stress distribution, the maximum tensile stress usually occurs below the surface. The fatigue failure may then initiate at this point of maximum stress.

This trend is especially true in carburized and nitrided parts, where the effect of the stress distribution is complemented by the change in material properties at the interface between the hard surface and the soft core.

A related trend is that residual compressive surface stresses will not significantly affect the fatigue strength of smooth axial specimens. This is because a smooth axial specimen has no stress gradient from applied loads. All the methods discussed for producing residual surface stresses will have the greatest effect in cases where there is a stress gradient due to applied loads. Examples of this are stress gradients due to bending, torsion, and notches.

Example 1.2

Several bars of high strength steel are to be used as leaf springs. These springs will be subjected to a zero-to-maximum ($R = 0$) three-point flexural loading. The bars are 1.50 in. wide and 0.192 in. thick. Half of the bars are in the "as-heat-treated" condition, while the other half have been shot peened. Determine the zero-to-maximum surface stress that will allow the bars to have an infinite life. The necessary data for the two sets of bars are given below. Use the Goodman relationship for these calculations.

As Heat Treated

Hardness = 48 Rockwell C ($\approx$ 465 BHN)

Residual surface stress = 0 ksi

Surface roughness (AA) = 24 μin.

Shot Peened

Hardness = 49 Rockwell C ($\approx$ 475 BHN)

Residual surface stress = −80 ksi

Surface roughness (AA) = 125 μin.

Solution First the calculations will be made for the as-heat-treated spring. The uncorrected endurance limit, S'_e, is found using Eq. (1.1). Since BHN > 400,

$$S'_e \approx 100 \text{ ksi}$$

The modification for size effect must take into account the fact that the cross-section of the bar is not round. Reference 5 suggests the following equation to determine the equivalent diameter, d_{eq}, for a rectangular section undergoing bending.

$$0.0766 d_{eq}^2 = 0.05bh$$

where b is the width and h thickness. Then

$$0.0766 d_{eq}^2 = 0.05(0.192 \text{ in.})(1.5 \text{ in.})$$
$$d_{eq} = 0.43 \text{ in.}$$

Using Eq. (1.13) (since $d_{eq} > 0.3$ in.) yields

$$C_{size} = 0.869(0.43)^{-0.097}$$

The modification factor for size is 0.94.

The modification factor for loading effect is 1.0 since the loading is reversed bending. The modification factor for surface finish requires that ultimate strength be known. The ultimate strength, S_u, of the spring can be estimated as

$$\begin{aligned} S_u &\approx 0.5(\text{BHN}) \\ &\approx 0.5(465) \\ &\approx 232\ \text{ksi} \end{aligned}$$

Reading from Fig. 1.14 at $S_u = 232$ ksi and AA $= 24\ \mu$in. the modification for surface roughness is 0.75.

Determine the modified endurance limit, S_e, using Eq. (1.12):

$$\begin{aligned} S_e &= S_e' \times \text{modification factors} \\ &= (100\ \text{ksi})(0.94)(1.0)(0.75) \\ &= 70.5\ \text{ksi} \end{aligned}$$

The next step is to determine the allowable stress for the spring by using the Goodman relationship [Eq. (1.9)]:

$$\frac{\sigma_a}{S_e} + \frac{\sigma_m}{S_u} = 1$$

For this case where loading is zero to maximum ($R = 0$), the mean stress, σ_m, and alternating stress, σ_a, are equal. Solving for the unknown gives us

$$\frac{\sigma}{70.5\ \text{ksi}} + \frac{\sigma}{232\ \text{ksi}} = 1$$

$$\sigma = \sigma_a = \sigma_m = 54\ \text{ksi}$$

$$\sigma_{max} = \sigma_a + \sigma_m = 108\ \text{ksi}$$

This would mean that for an infinite life the outer surface of the spring could cycle between 0 and 108 ksi. Test results indicate that the actual value is 0 to 100 ksi. The analysis provides an answer with an 8% nonconservative error.

Next are the calculations for the shot peened spring. The uncorrected endurance limit, S_e', and the modifications for size and loading would be the same as for the as-heat-treated spring.

The modification factor for surface finish requires a value for ultimate strength.

$$\begin{aligned} S_u &\approx 0.5(\text{BHN}) \\ &\approx 0.5(475) \\ &\approx 238\ \text{ksi} \end{aligned}$$

Reading from Fig. 1.14 at $S_u = 238$ ksi and AA $= 124\ \mu$in. the modification for surface roughness is 0.58.

Determine the modified endurance limit, S_e.

$$S_e = (100 \text{ ksi})(0.94)(1.0)(0.58)$$
$$= 54.5 \text{ ksi}$$

It is necessary to include a modification for the residual surface stress. The residual surface stress (-80 ksi) can be accounted for in the Goodman equation since the residual stress can be combined with the imposed mean stress. The allowable stress is determined by using the relationship [Eq. (1.9)]

$$\frac{\sigma_a}{S_e} + \frac{\sigma_m}{S_u} = 1$$

For this case, where loading is zero to maximum ($R = 0$), the mean stress, σ_m, and alternating stress, σ_a, are equal, but the equation must also take into account the residual surface stress. This value will be combined with the mean stress. Solving for the unknown, we obtain

$$\frac{\sigma}{54.5 \text{ ksi}} + \frac{\sigma - 80}{238 \text{ ksi}} = 1$$

$$\sigma = \sigma_a = \sigma_m = 59.3 \text{ ksi}$$

$$\sigma_{\max} = \sigma_a + \sigma_m = 118.6 \text{ ksi}$$

Therefore, for an infinite life, the outer surface of the shot peened spring could cycle between 0 and 118.6 ksi. Test results indicate that the actual value is 0 to 140 ksi. The analysis provides an answer with a 15% conservative error.

One effect that was not considered in this analysis was that shot peening increases the uncorrected endurance limit (see Fig. 1.24). It should be noted that the beneficial effect of the compressive residual stress caused by shot peening more than offsets the detrimental increase in surface roughness. Another point which should be considered is that since the maximum surface stress is well below the yield strength of the material, there should be no problem with relaxation of residual stresses. (Data for this problem were taken from Ref. 14.)

1.4.5 Temperature

There is a tendency for the endurance limits of steels to increase at low temperatures. A more important design consideration, however, is that many materials experience a significant reduction in fracture toughness at low temperatures.

At high temperatures the endurance limit for steels disappears due to the mobilizing of dislocations. At temperatures beyond approximately one-half of the melting point of the material, creep becomes important. In this range the stress–life approach is no longer applicable. It is also important to note that high temperatures can cause annealing, which may remove beneficial residual compressive stresses.

1.4.6 Environment

When fatigue loading takes place in a corrosive environment the resulting detrimental effects are more significant than would be predicted by considering fatigue and corrosion separately. The interaction of fatigue and corrosion, which is called corrosion-fatigue, involves unique failure mechanisms which are very complex. The work in this area is still very much at the research stage and very little is available in the way of quantified data or useful theories.

The basic mechanism of corrosion-fatigue during the initiation stage can be explained this way. A corrosive environment attacks the surface of a metal and produces an oxide film. Usually, this oxide film would serve as a protective layer and prevent further corrosion of the metal. However, cyclic loading causes localized cracking of this layer, which exposes fresh metal surfaces to the corrosive environment. At the same time corrosion causes localized pitting of the surface, and these pits serve as stress concentrations. The mechanism of corrosion-fatigue during the crack propagation stage is very complicated and not well understood.

One of the main difficulties in trying to quantify corrosion-fatigue is the large number of variables involved in testing. Consider the corrosion-fatigue of the important combination of steel in water. Some of the variables that must be considered are alloying elements in the steel, chemical makeup of the water, temperature, degree of aeration, flow velocity, and salt content. One of the many trends is that corrosion-fatigue is much worse in a spray than when the metal is fully immersed. Another variable that is very critical is loading frequency. Fatigue tests in noncorrosive environments can be run at almost any frequency and similar data will be obtained. On the other hand, corrosion-fatigue data are greatly influenced by loading frequency. Low frequency tests allow more time for corrosion to take place, and resulting fatigue lives are shorter.

There are some general trends observed in corrosion-fatigue. Figure 1.25 shows the generalized S–N curves for steel in four different environments. The curves generated in room air and a vacuum show that even the humidity and oxygen in room air can slightly reduce fatigue strength. The curve for presoak involves the case where the steel is soaked in a corrosive environment and then the fatigue test is run in room air. The reduction of fatigue properties for this curve is due to the rough surface caused by corrosion pitting. The curve for corrosion-fatigue is significantly below the one for room air. Another trend is that corrosion-fatigue eliminates the endurance limit behavior seen in many steels.

Another important trend is shown in Fig. 1.26, which shows the endurance limit for various steels in room air and freshwater environments. The data for plain carbon steels indicate that higher strength steels have no advantage in a corrosive environment. Note that steels with a high chromium content have icial residual com-

nent the resulting
ted by considering
d corrosion, which
ms which are very
rch stage and very
es.
tiation stage can be
ace of a metal and
s a protective layer
clic loading causes
al surfaces to the
alized pitting of the
The mechanism of
omplicated and not

osion-fatigue is the
corrosion-fatigue of
riables that must be
keup of the water,
nt. One of the many
n when the metal is
g frequency. Fatigue
any frequency and
ion-fatigue data are
allow more time for
r.
fatigue. Figure 1.25
t environments. The
n the humidity and
e curve for presoak
vironment and then
e properties for this
tting. The curve for
Another trend is that
n in many steels.
shows the endurance
ments. The data for
e no advantage in a
mium content have

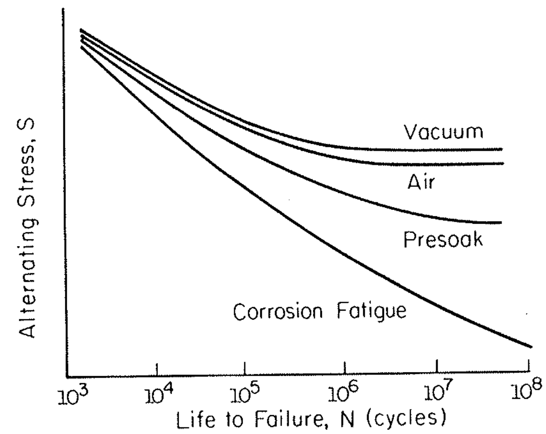

Figure 1.25 Effect of various environments on the *S–N* curve of steel. (H. O. Fuchs and R. I. Stephens, *Metal Fatigue in Engineering,* John Wiley and Sons, New York, 1980. Reprinted with permission.)

significantly better corrosion-fatigue resistance than that of plain carbon steels. A general trend is that materials which are resistant to corrosion alone will also have good corrosion-fatigue properties.

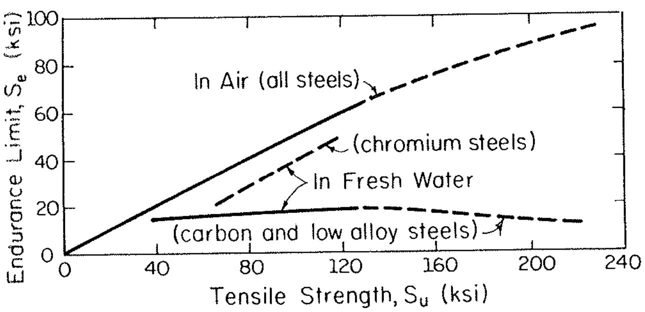

Figure 1.26 Influence of tensile strength and chemical composition on corrosion-fatigue strength of steels. (From Ref. 10.)

There are several methods that can be used to reduce the problems caused by corrosion-fatigue. Perhaps the most effective is to use a steel with a high chrome content. Table 1.6 compares the fatigue properties of a plain carbon and chromium steel in salt water.

TABLE 1.6 Fatigue Strength of Steels in Corrosive Environment[a]

Material	S_u (ksi)	Endurance Limit[b] (ksi) In Air	Endurance Limit[b] (ksi) In Salt Water	Percent Reduction
SAE 1050	116	53.8	22.6	58
5% Cr steel	116	66	47.2	28

[a] 6.8% Salt water, complete immersion.
[b] Basis for endurance limit in corrosive environment is 10^7 cycles.
Source: Ref. 10.

TABLE 1.7 Effect of Various Surface Treatments on the Corrosion Fatigue of Mild Steel

		Endurance Limit[a] (ksi)			
		In Air		In Fresh Water	
S_u (ksi)	Surface Treatment	Untreated	Treated	Untreated	Treated
53	Cold rolling	33	37	13	19
50	Nickel plate	28	20	14	20
50	Cadmium coat	28	29	14	22

[a] Basis for endurance limit in corrosive environment is 10^8 cycles.

Source: Ref. 10.

There are several surface treatments that will improve corrosion-fatigue resistance. Examples of these are shown in Table 1.7. Surface coatings such as paint, and platings using chrome, nickel, cadmium, or zinc, are useful. Note that nickel plating causes a reduction of fatigue strength in air but gives improvement in a corrosive environment. An advantage in using a softer metal for a coating is that it is more likely to remain intact when a crack forms in the base metal. One problem with surface coatings is that fatigue cracks can start at even the smallest break in a coating.

Surface treatments that produce compressive residual surface stresses (nitriding, shot peening, cold rolling, etc.) are also useful. These treatments cause the maximum tensile stress to occur below the surface. The reverse is also true and tensile residual surface stresses are very detrimental and promotes corrosion-fatigue.

1.5 IMPORTANT CONCEPTS

- Care should be taken when using the idea of an endurance limit, a "safe stress" below which fatigue will not occur. Only plain carbon and low-alloy steels exhibit this property, and it may disappear due to high temperatures, corrosive environments, and periodic overloads.
- As a general trend the following factors will reduce the value of endurance limit:
  Tensile mean stress
  Large section size
  Rough surface finish
  Chrome and nickel plating
  Decarburization (due to forging and hot rolling)
  Severe grinding
- The following factors tend to increase the endurance limit:
  Nitriding

Flame and induction hardening
Carburization
Shot peening
Cold rolling

1.6 IMPORTANT EQUATIONS

Endurance Limit Related to Hardness

$$S_e(\text{ksi}) \approx 0.25 \times \text{BHN} \quad \text{for BHN} \leq 400$$
$$\text{if} \quad \text{BHN} > 400,\ S_e \approx 100\ \text{ksi} \tag{1.1}$$

where BHN is the Brinell hardness number

Endurance Limit Related to Ultimate Strength

$$S_e \approx 0.5 \times S_u \quad \text{for } S_u \leq 200\ \text{ksi}$$
$$\text{if} \quad S_u > 200\ \text{ksi},\ Se \approx 100\ \text{ksi} \tag{1.2}$$

Alternating Stress Relationships

$$\Delta\sigma = \sigma_{\max} - \sigma_{\min} = \text{stress range}$$

$$\sigma_a = \frac{\sigma_{\max} - \sigma_{\min}}{2} = \text{stress amplitude}$$

$$\sigma_m = \frac{\sigma_{\max} + \sigma_{\min}}{2} = \text{mean stress}$$

$$R = \frac{\sigma_{\min}}{\sigma_{\max}} = \text{stress ratio}$$

$$A = \frac{\sigma_a}{\sigma_m} = \text{amplitude ratio}$$

R and A Values Corresponding to Common Loading Situations

Fully reversed:	$R = -1$	$A = \infty$
Zero to maximum:	$R = 0$	$A = 1$
Zero to minimum:	$R = \infty$	$A = -1$

Mean Stress Correction Relationships

Soderberg (USA, 1930): $$\frac{\sigma_a}{S_e} + \frac{\sigma_m}{S_y} = 1 \tag{1.8}$$

$$\text{Goodman (England, 1899):} \quad \frac{\sigma_a}{S_e} + \frac{\sigma_m}{S_u} = 1 \tag{1.9}$$

$$\text{Gerber (Germany, 1874):} \quad \frac{\sigma_a}{S_e} + \left(\frac{\sigma_m}{S_u}\right)^2 = 1 \tag{1.10}$$

$$\text{Morrow (USA, 1960s):} \quad \frac{\sigma_a}{S_e} + \frac{\sigma_m}{\sigma_f} = 1 \tag{1.11}$$

Relationship between S_e under Various Loading

$$S_e(\text{axial}) \approx 0.70 S_e(\text{bending}) \tag{1.15}$$

$$\tau_e(\text{torsion}) \approx 0.577 S_e(\text{bending}) \tag{1.16}$$

REFERENCES

1. C. C. Osgood, *Fatigue Design,* 2nd ed., Pergamon Press, Oxford, 1982.
2. U.S. Department of Defense, MIL-HBDK-5.
3. G. Sines and J. L. Waisman, (eds.), *Metal Fatigue,* McGraw-Hill, New York, 1959.
4. J. H. Faupel and F. E. Fisher, *Engineering Design,* Wiley-Interscience, New York, 1981.
5. J. E. Shigley and L. D. Mitchell, *Mechanical Engineering Design,* 4th ed., McGraw-Hill, New York, 1983.
6. R. C. Juvinall, *Engineering Considerations of Stress, Strain, and Strength,* McGraw-Hill, New York, 1967.
7. R. C. Johnson, *Mach. Des.*, Vol. 45, No. 11, 108, 1973.
8. H. O. Fuchs and R. I. Stephens, *Metal Fatigue in Engineering,* Wiley-Interscience, New York, 1980.
9. J. O. Almen and P. H. Black, *Residual Stresses and Fatigue in Metals,* McGraw-Hill, New York, 1963.
10. P. G. Forrest, *Fatigue of Metals,* Pergamon Press, Oxford, 1962.
11. L. P. Tarasov and H. J. Grover, "Effect of Grinding and Other Finishing Processes on the Fatigue Strength of Hardened Steel," *Am. Soc. Test. Mater. Proc.*, Vol. 50, 1950, p. 668.
12. J. C. Straub, "Shot-Peening," in *Metals, Engineering, Design,* 2nd ed., O. J. Horger (ed.), McGraw-Hill, New York, 1965, p. 258.
13. O. J. Horger, "Mechanical and Metallurgical Advantages of Shot-Peening," *Iron Age,* March 29 and April 5, 1945.
14. R. L. Mattson and J. G. Roberts, "The Effect of Residual Stresses Induced by Strain Peening upon Fatigue Strength," in *Internal Stresses and Fatigue in Metals,* G. M. Rossweiler and W. L. Grube, (eds.), Elsevier, New York, 1959, pp. 337–357.
15. H. F. Moore and J. B. Kommers, "An Investigation of the Fatigue of Metals," *Univ. Ill. Eng. Exp. Stn. Bull.*, 124, 1921.

16. H. F. Moore and T. M. Jasper, "An Investigation of the Fatigue of Metals," *Univ. Ill. Eng. Exp. Stn. Bull.*, 136, 1923.
17. J. A. Graham, (ed.), *Fatigue Design Handbook*, Society of Automotive Engineers, Warrendale, Pa., 1968.
18. J. O. Smith, "The Effect of Range of Stress on the Torsional Fatigue Strength of Steel," *Univ. Ill. Eng. Exp. Stn. Bull.*, 316, 1939.
19. R. Kuguel, "A Relation between Theoretical Stress Concentration Factor and Fatigue Notch Factor Deduced from the Concept of Highly Stressed Volume," *Am. Soc. Test. Mater. Proc.*, Vol. 61, 1961, pp. 732–748.
20. H. F. Moore and T. M. Jasper, "An Investigation of the Fatigue of Metals," *Univ. Ill. Eng. Exp. Stn. Bull.*, 142, 1924.
21. R. Cazaud, *Fatigue of Metals*, Philosophical Library, New York, 1953.
22. G. E. Dieter, *Mechanical Metallurgy*, 3rd ed., McGraw-Hill, New York, 1986.
23. A. F. Madayag, (ed.), *Metal Fatigue: Theory and Design*, Wiley, New York, 1969.
24. J. A. Collins, *Failure of Materials in Mechanical Design*, Wiley-Interscience, New York, 1981.
25. C. Lipson and N. J. Sheth, *Statistical Design and Analysis of Engineering Experiments*, McGraw-Hill, New York, 1973.
26. E. B. Haugen, *Probabilistic Mechanical Design*, Wiley-Interscience, New York, 1980.
27. L. Sors, *Fatigue Design of Machine Components*, Pergamon Press, Oxford, 1971.

References 1, 6, 8, 17, and 23 are general fatigue design texts or handbooks with several chapters devoted to the stress-life approach. Reference 6 is especially recommended.

References 4, 5, 22, and 24 are general design and materials texts with chapters devoted to fatigue.

References 3, 10, 21, and 27 give surveys of fatigue technology current to 1950, 1960, and 1970. Each has extensive lists of references. Reference 10 is a British perspective. References 21 and 27 were written by European authors.

Reference 9 deals with residual stresses, shot peening, and cold rolling.

References 25 and 26 deal with the statistical and probabilistic design aspects of fatigue.

PROBLEMS

SECTION 1.2

1.1. Given a steel with an ultimate strength of 100 ksi, estimate the allowable alternating stress for lives of 10^3, 10^4, 10^5, and 10^6 cycles. Solve this problem using the graphical method shown in Fig. 1.5 and Eq. (1.7). Repeat this procedure for a steel with an ultimate strength of 220 ksi.

1.2. Given below are the monotonic and rotating bending fatigue test data for three steels. Plot the fatigue data on log-log coordinates. Compare the test data to the estimate of the S–N curve made using the method shown in Fig. 1.5. (Data taken from Ref. 15.)